Molecular Crystals and Liquid Crystals

Publication details, including instructions for authors and subscription information:
http://www.tandfonline.com/loi/gmcl20

Surface Treatments for Lyotropic Liquid Crystals Alignment

I. H. Bechtold [a], M. L. Vega [a], E. A. Oliveira [a] & J. J. Bonvent [b]

[a] Instituto de Física, Universidade de São Paulo, P.O. Box 66318, São Paulo, SP, 05389-970, Brazil

[b] Universidade de Mogi das Cruzes, Av. Dr. Cândido Xavier de Almeida Souza, 200, Mogi das Cruzes, SP, 08780-911, Brazil

Version of record first published: 18 Oct 2010

To cite this article: I. H. Bechtold, M. L. Vega, E. A. Oliveira & J. J. Bonvent (2002): Surface Treatments for Lyotropic Liquid Crystals Alignment, Molecular Crystals and Liquid Crystals, 391:1, 95-110

To link to this article: http://dx.doi.org/10.1080/10587250216175

Mol. Cryst. Liq. Cryst., Vol. 391, pp. 95–110

1542-1406/03 $12.00 + .00
DOI: 10.1080/15421400390193585

Taylor & Francis
Taylor & Francis Group

SURFACE TREATMENTS FOR LYOTROPIC LIQUID CRYSTALS ALIGNMENT

*I. H. Bechtold, M. L. Vega and E. A. Oliveira**
Instituto de Física, Universidade de São Paulo,
P.O. Box 66318, São Paulo, 05389-970, SP, Brazil

J. J. Bonvent
Universidade de Mogi das Cruzes, Av. Dr. Cândido Xavier de Almeida Souza, 200, 08780-911, Mogi das Cruzes—SP, Brazil

For nematic lyotropic liquid crystals it has been experimentally observed that in nontreated glass cells the director in the surface layer can be reoriented by a magnetic field in any direction parallel to the surface, and the final state is stable. In this paper we will focus on the equilibrium configuration of the director in the surface layer in the presence of a magnetic field, using cells with treated surfaces to introduce an easy axis. The surface treatments employed in this study are: rubbing of glass plates coated with polymer (PMMA), rubbing of bare glass plates, and unidirectional deposition of Teflon. All these surface treatments induce a preferential orientation to the liquid crystal. From AFM analysis we observe microchannels in the polymer films that are more homogeneous for the Teflon film. The experimental results indicate that the anchoring energy depends on the surface treatment and is larger for the rubbed glass plates.

Keywords: lyotropic liquid crystal; surface treatment; anchoring energy; dynamical process; equilibrium states

INTRODUCTION

The surface-induced bulk alignment of thermotropic liquid crystals (TLC) is of great importance for LC display technology. Although many theoretical and experimental studies have been performed on this subject by many

Received 19 August 2002; accepted 30 October 2002.

The authors are grateful to Prof. Roberto Mendonça Faria, Tech. Marcelo A.P. da Silva (IF/USP–São Carlos), to the "Laboratório de Filmes Finos do IF/USP—São Paulo, (FAPESP Proc.#95/5651-0)" for the SPM facility, and to FAPESP for the financial support.

*Corresponding author. Fax: 11-3814-0503.

researchers in recent years, the alignment mechanisms are not completely understood [1,2]. With regard to lyotropic liquid crystals (LLC) we deal with a more complex system, and the anchoring properties seem to be quite different from those found in TLC [3]. In a nematic LLC two different orientation processes have been identified when a magnetic field **H** is applied; a fast one related to the orientation of the director in the bulk, and a slow one related to the orientation of the director in the surface layer. One of the particularities of the LLC is the possibility of the director gliding in the surface layer. Experimentally, it has been observed that in isotropic glass cells the director in the surface layer can be oriented in any direction parallel to the surface. The direction can be changed by rotating the field direction, and the final state is stable, i.e., the orientation induced by the magnetic field remains when the magnetic field is removed. For an isotropic substrate there is no positional anchoring such as is found in thermotropics, and the micelles can glide in the plane parallel to the substrate or rotate around the axis perpendicular to it. The effect of the substrate consists mainly of suppressing the micellar fluctuation around the axes parallel to the boundary surface.

The reorientation process of the director in the surface layer for a lyotropic liquid crystal is satisfactorily described by a phenomenological model that considers the existence of a biaxial surface layer of finite thickness interacting directly with the magnetic field, resulting in a characteristic time for the reorientation process which is proportional to H^{-2}. A detailed experimental investigation of the dynamic behavior of such a process was carried out using cells where the inner surfaces were treated to induce a preferential orientation of the micelles [4].

In this article, we will focus on the equilibrium configuration of the director in the surface layer in the presence of a magnetic field using cells with treated surfaces to introduce an easy axis. Therefore, the final orientation of the director in the surface layer results from a competition between the interactions of the liquid crystal with the treated substrate and the magnetic field. The surface treatments employed are; (1) rubbing of glass plates and glass plates coated with a polymer film and (2) unidirectional deposition of Teflon. The topography of the treated substrates was analyzed by means of atomic force microscopy (AFM). The purpose of such analysis is to investigate the correlation between the surface topography and the induced alignment to the liquid crystalline matrix.

REORIENTATION OF THE DIRECTOR IN THE SURFACE LAYER

In this section we will briefly present the phenomenological models that have been proposed to describe the dynamical reorientation process of the

director in the surface layer [5] and the equilibrium states in the presence of the magnetic field [6,7]. Only the main assumptions and equations related to the analysis carried out in this paper will be discussed.

Dynamical Process

The nematic lyotropic liquid is constituted of biaxial micelles and characterized by three symmetry axes. In contact with an isotropic boundary surface, the spatial fluctuations of the micelles will be restricted, and as a consequence the orientation of the director perpendicular to the surface is fixed. If a magnetic field (**H**) is applied to the lyotropic nematic sample parallel to the substrate, the micelles tend to align with their longest axis along the field direction **H**, leading to the formation of a biaxial layer of finite thickness, with two-dimensional orientation order, interacting directly with the magnetic field. The orientational order in the surface layer and in the bulk will be characterized by the order parameters ρ and r, respectively.

Let us consider a semi-infinite sample with the boundary surface located at $z = 0$ and initially oriented parallel to the x axis. The magnetic field **H** is applied to the sample, making an angle θ with respect to the x axis, resulting in a twist distortion of the director in the bulk given by $\varphi(z)$, which is the angle between the director and the x axis. Since the orientation of the director in the bulk is much faster than in the surface layer [3], we will consider the initial state as a distorted one, and we will assume that far from the boundary surface the director orients parallel to the magnetic field; $\varphi(z \to \infty) = \theta$. In the surface layer the orientation of the director will be described by the angle between the director and the x axis, $\Phi(t)$.

The free energy of the system (per unity area) can be written as the sum of the contributions of the bulk elastic energy in the presence of the magnetic field and the contribution of the surface layer interacting with both the magnetic field and the bulk [5]:

$$f = F_{V0} + F_{S0} + \frac{1}{2}\int_0^\infty K\left(\frac{d\varphi}{dz}\right)^2 + \frac{1}{2}\int_0^\infty \chi_a H^2 \cos^2(\theta - \varphi)dz$$

$$-\frac{1}{2}DH^2\rho\cos^2\Phi - Cr\rho\cos^2(\Phi - \varphi_0) \qquad (1)$$

where K is the twist elastic constant, χ_a is the anisotropy of the diamagnetic susceptibility, C and D are phenomenological constants that characterize the interactions of the surface layer with the bulk and with the magnetic field, respectively, and φ_0 gives the orientation of the director in the interface, $\varphi(z \to 0) = \varphi_0$.

The time evolution of the director orientation in the surface layer is obtained from the Landau-Khalatnikov equations and is given by

$$\Phi(t) = \theta(1 - \exp(-t/\tau)) \tag{2}$$

where τ is the characteristic time of the surface reorientation process and is proportional to H^{-2}.

For small deformations; sin $\varphi \approx \varphi$, the orientation of the director in the bulk can be obtained by imposing the equilibrium of the elastic and magnetic torques in Equation (1), resulting in:

$$\varphi(z) = \theta - 2\arctan\left[\exp(-z/\xi)\tan\left(\frac{\theta - \varphi_0}{2}\right)\right] \tag{3}$$

where ξ is the magnetic correlation length, $\xi = (K/\chi_a)^{1/2}/H$. From the balance of the torque in the bulk we obtain the orientation of the director in the interface:

$$\varphi_0 = \frac{\Phi - h\theta}{1 - h} \tag{4}$$

with $h = H/H_0$, and $H_0 = (K\chi_a)^{1/2}/(2Cr\rho)$. The above equation shows that φ_0 depends on $\Phi(t)$, which means that the boundary condition close to the surface is time dependent.

Equilibrium States

It has been experimentally observed that, for LLC in contact with non-treated surfaces, there is a critical magnetic field (H_c^*), above which an irreversible deformation of the surface layer occurs [6]. The fitting of the experimental curves of transmittance for different magnetic field intensities allowed the determination of the final orientation of the director in the surface layer $\varphi_f(H)$. Such a curve exhibited a saturation regime; the director tends to align parallel to the magnetic field direction for increasing field intensity, but this regime is reached with a discontinuity, at a second critical magnetic field (H_c^{**}). A phenomenological model has been proposed, considering the interaction between the surface layer and the substrate by means of a dry–friction-like energy and an elastic interaction between the bulk and surface layer. This model predicts the existence of the second critical magnetic field H_c^{**}, above which the torque at the interface is larger than the critical torque, and the elastic coupling between the surface layer and the bulk is broken. According to this model the orientation of the director in the surface layer, for $H_c^* < H < H_c^{**}$ is given by [7]:

$$\frac{w}{2}\sin(2\varphi_f) + \Gamma_c - \frac{u}{1 + u\left(\frac{l}{K_s} + \frac{\xi}{K}\right)}(\theta - \varphi_f) = 0 \tag{5}$$

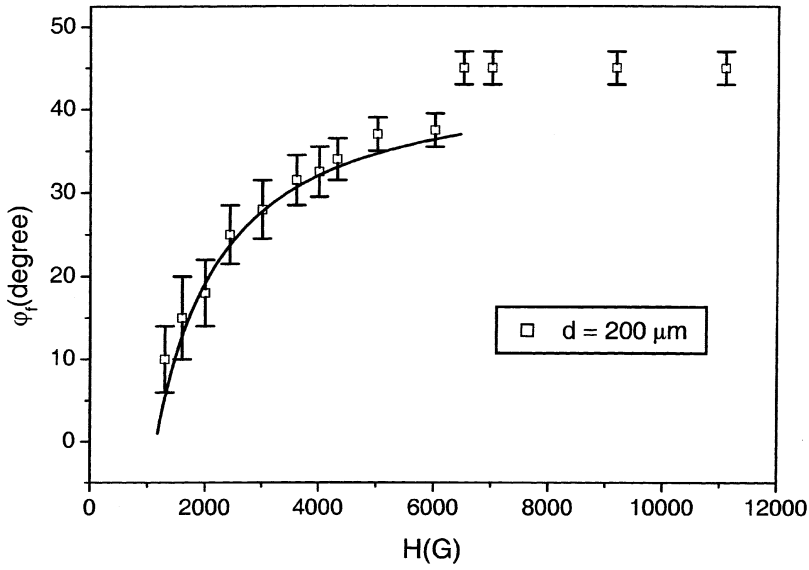

FIGURE 1 Equilibrium orientation of the director in the surface layer as a function of the magnetic field for nontreated boundary surfaces (glass capillaries, VitroDynamics) 200 μm thick. The solid line corresponds to the fitting using Equation (5), taking u, w, and l as fitting parameters. From the best fitting the values obtained are: $w = 10^{-9}$ erg/cm^2, $u = 1$ erg/cm^2 and $l = 10^{-6}$ cm.

where w is the dry–friction-like energy; $\Gamma_c = (K/\xi_c^*)\sin\theta$ is the critical torque related to the first critical magnetic field (H_c^*); K_s is the elastic constant in the surface layer, l is the thickness of the surface layer, and u is the elastic coupling constant between the surface layer and the bulk. Equation (5) was successfully applied to fit the experimental values of $\varphi_f(H)$ obtained for nontreated boundary surfaces, as is shown in Figure 1.

EXPERIMENT

The LLC system investigated is a ternary mixture composed of ionic surfactants; 35.3 wt% of potassium laruate (KL), 4 wt% of decylammonium chloride (DaCl), and 60.7 wt% of water. The solution presents a hexagonal phase and two uniaxial nematic phases (calamitic N_c and discotic N_d) separated by a biaxial phase N_{bx}. The phase transitions differ from each other only by orientational fluctuations around the symmetry axes of the micelles [8,9]. The transition temperatures were precisely determined by birefringence measurements as a function of the temperature: H_α–N_c at 15°C, N_c–N_{bx} at 30°C, and N_{bx}–N_d at 35°C.

The lyotropic material was inserted into glass cells of different thicknesses (10, 50, and 200 μm). The cells were built by sealing two treated glass plates that were kept distant by Mylar spacers of a given thickness. The glass plates (15 mm of width and 25 mm of length) were first carefully cleaned before any specific surface treatment. In this study different treatments were applied to the boundary surfaces: rubbing of glass plates, rubbing of glass plates coated with a polymer film, and unidirectional deposition of Teflon. Unidirectional rubbing was performed by means of a homemade machine which consists of a cylinder covered with soft velvet rolling on the substrates. The gliding velocity and the pressure of the cylinder on the substrates are controlled. The polymer film is the poly-methyl-methacrylate (PMMA) drawn by spin coating on the glass plates. For the Teflon deposition, a Teflon bar is glided upon the glass substrate heated up to 150°C. The purpose of such treatments is to create an easy axis ($\mathbf{n}_0$), which is the rubbing direction in the case of the rubbed surfaces and the gliding direction in the case of the Teflon. Images of the treated surfaces were acquired by AFM using a Nanoscope IIIa (Digital Instruments) in contact mode, at 2.97 Hz scanning rate and 256×256 lines.

The cells are prepared in order to have planar alignment, with the surface of the substrates parallel to each other. The liquid crystal is introduced by capillary action at room temperature (≈ 22°C), i.e., with the sample in the nematic calamitic phase, and then sealed with UV curable adhesive (3M). The cells were then observed with a polarizing microscope to check the induced alignment.

To probe the surface effects we induce a reorientation process by applying a magnetic field to an initial uniformly oriented sample. We follow the reorientation process by measuring the intensity of transmitted light through the sample as a function of time when the magnetic field is applied. The experimental setup for the transmittance measurements consists basically of an incident laser beam along the z axis, linearly polarized, crossing successively the LC sample, a photoelastic modulator (PEM), and a second polarizer disposed at crossed direction with respect to the first one, before hitting a photodetector (Figure 2). The sample is initially oriented along the easy axis $\mathbf{n}_0$, and such condition is fulfilled by applying a strong magnetic field parallel to $\mathbf{n}_0$, even for those samples which exhibit spontaneous alignment induced by the boundary surfaces.

The propagation of light through the optical elements as well as through the nematic sample is simulated using the Jone's matrix method. We consider that the nematic sample can be divided in many thin layers with uniform orientation in each layer, where a phase shift and a rotation of the polarization direction takes place [10]. For a semi-infinite sample, the evolution of the director in the surface layer and in the bulk is described by Equations (2) and (3), respectively. However, we have to adapt the

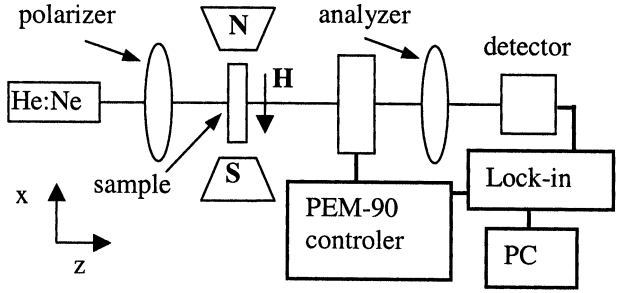

FIGURE 2 Experimental setup used to measure the transmittance of the nematic sample as a function of the time when the magnetic field is applied.

equations to match the boundary conditions of a finite sample. Considering equivalent surfaces located at $z = 0$ and $z = d$, we assume that the profile of the director is symmetrical and must satisfy the following boundary conditions: for low magnetic fields, in the middle of the sample ($z = d/2$) the orientation of the director is not necessary parallel to **H**. Therefore, Equation (3) can be used to describe the twist of the director for $0 \leq z \leq d/2$, replacing θ by φ_f in Equations (2) and (3). The experimental curves of transmittance can then be fitted taking τ and φ_f as the fitting parameters. It is important to note that such equations result in a final state that is homogeneous, i.e., the director is oriented making an angle φ_f with respect to x axis, which depends on the intensity of the magnetic field, $\varphi_f = \varphi_f(H)$. If the director in the surface layer is free to glide, we expect that $\varphi_f = \theta$, but since there is an easy axis in the boundary surfaces, the final orientation may be different from the orientation imposed by the magnetic field.

EXPERIMENTAL RESULTS AND DISCUSSIONS

The Topography of the Substrates

The surface morphology of a rubbed glass plate and a rubbed PMMA-coated plate is presented in Figures 3(a) and 3(b), respectively. It can clearly be observed that the glass substrate presents a lower value for the mean roughness—$R_M = 0.22$ nm, compared to that of the PMMA-treated substrate ($R_M = 1.66$ nm)—and that for the bare glass rubbing does not provoke any significant surface deformation such as microgrooves. It is important to remember that a soft velvet cloth was used to rub the substrates.

Regarding the rubbed PMMA substrate, we observe the formation of microgrooves (Figure 3(b)) about 0.04 μm wide along the rubbing

direction. In the case of substrate coated with Teflon, we observe the presence of microgrooves about 0.3 μm wide and 2.5 nm high, aligned along the Teflon deposition direction, and the mean roughness is $R_M = 2.04$ nm. We can also notice that the distribution of microgrooves is more homogeneous than on rubbed PMMA (see Figure 3(c)).

The aligning efficiency of the treated substrates was first analyzed by direct observation of the resulting textures of the nematic LLC sandwiched between two identically treated substrates, by means of a polarizing microscope. It was found that a spontaneous homogeneous alignment can be achieved along the surface-imposed aligning direction ($\mathbf{n}_0$) only if the lyotropic material is confined within cell as thin as 10 μm. For samples 200 μm and 50 μm thick the texture indicates a degenerated planar alignment. A homogeneous alignment can be improved when a strong magnetic field (typically 10 kG) is applied in the same direction as the rubbing or Teflon deposition during approximately 1 h. Nevertheless, if the boundary surfaces are not treated, no uniform alignment can be obtained even after more than 5 h of exposure to the magnetic field. It means that a certain anisotropy in

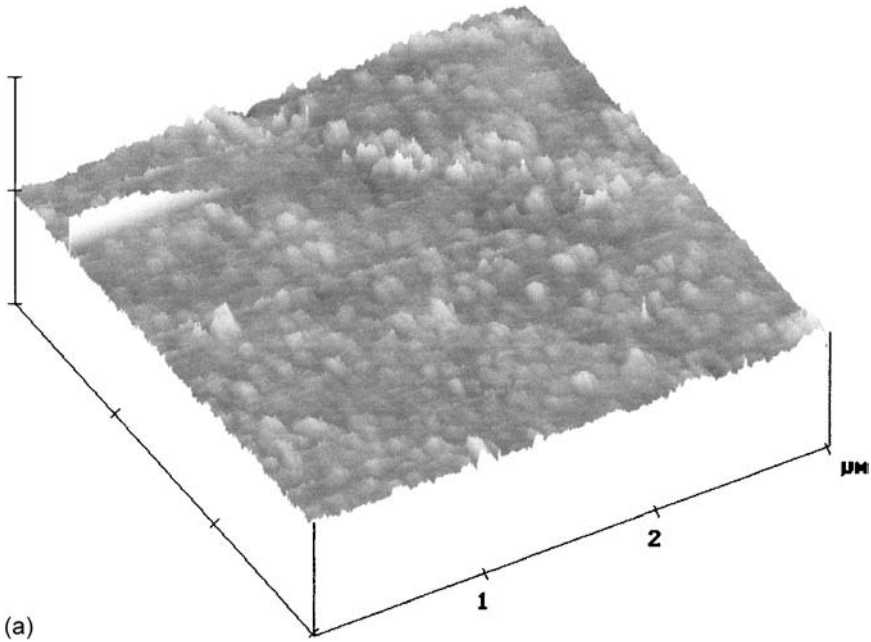

FIGURE 3 AFM images of the substrate used in the cell's confection. (a) bare glass, (b) rubbed PMMA, and (c) Teflon deposition surface. The vertical scale is the same for all figures; $z = 10$ nm.

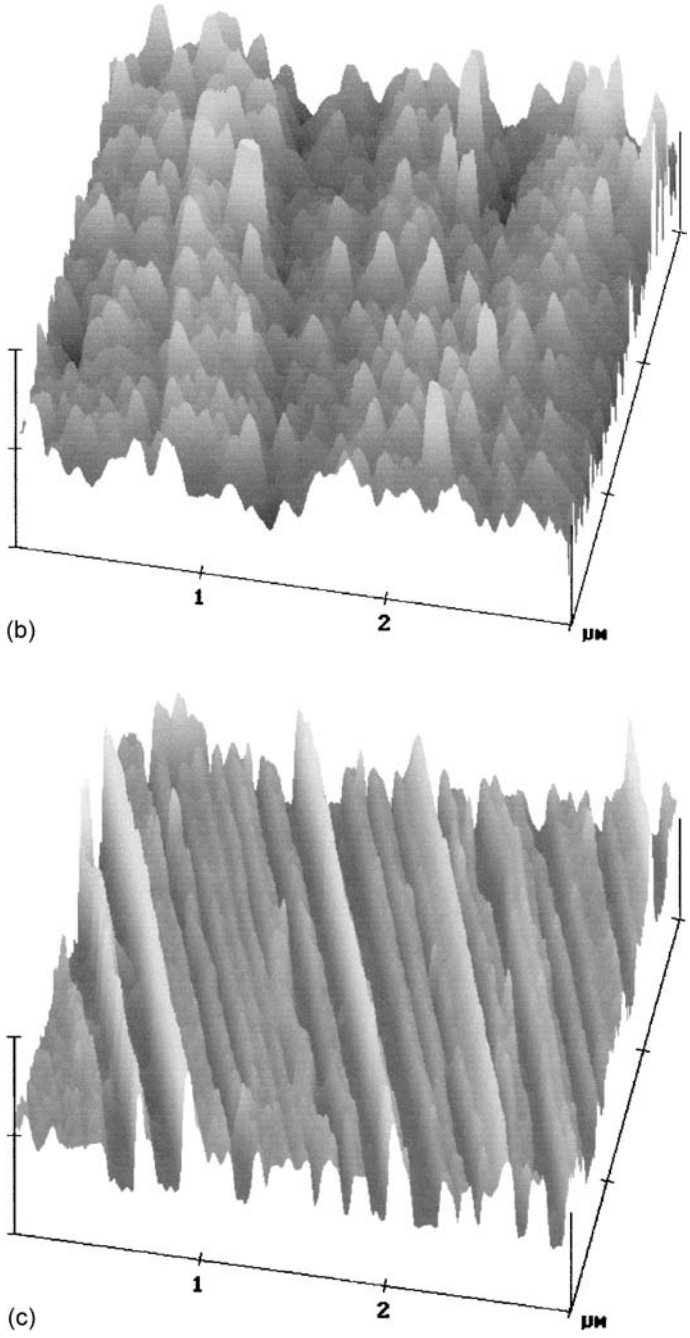

FIGURE 3 (*Continued.*)

the boundary surfaces is necessary to promote the orientation of the director in a preferential direction. Furthermore, surprisingly, no significant difference could be observed when comparing the LC textures with the different treated substrates. Therefore, observations of textures are not enough to distinguish between different surface treatments.

Transmittance Measurements

Transmittance curves for the reorientation of the surface director are presented in Figure 4(a) when a strong magnetic field ($H \approx 10\,kG$) is applied. The influence of the sample thickness is investigated by using cells 10, 50, and 200 μm thick, built with the same substrate—rubbed PMMA-coated glass plates. For the thickest sample (200 μm) there is a saturation level which corresponds to the final equilibrium state. The saturation plateau is related to the maximum director distortion induced by the magnetic field, and it can be seen that for the thinner samples (10 and 50 μm) the transmittance stabilizes at a lower value, which is related to a smaller deformation. Texture observations of such samples, exposed to magnetic field for a long time ($t \gg \tau_s$), have shown that there is a uniform orientation

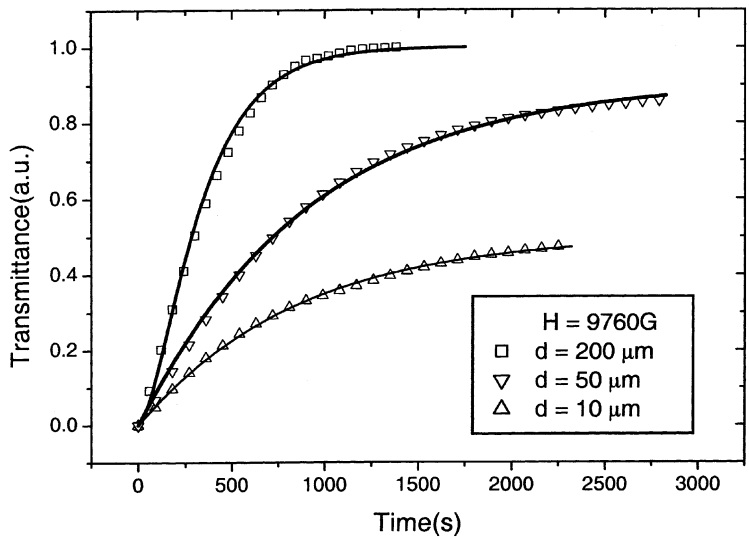

FIGURE 4 Experimental curves of the transmittance of a NLLC material sandwiched (a) in cells of different thicknesses (10, 50, and 200 μm) and (b) in cells of 10 μm thick for different surface treatments. Figure 4(a) comes from Bechtold et al. [4], and the solid lines correspond to the fitting curves for the two director profiles discussed in the present text.

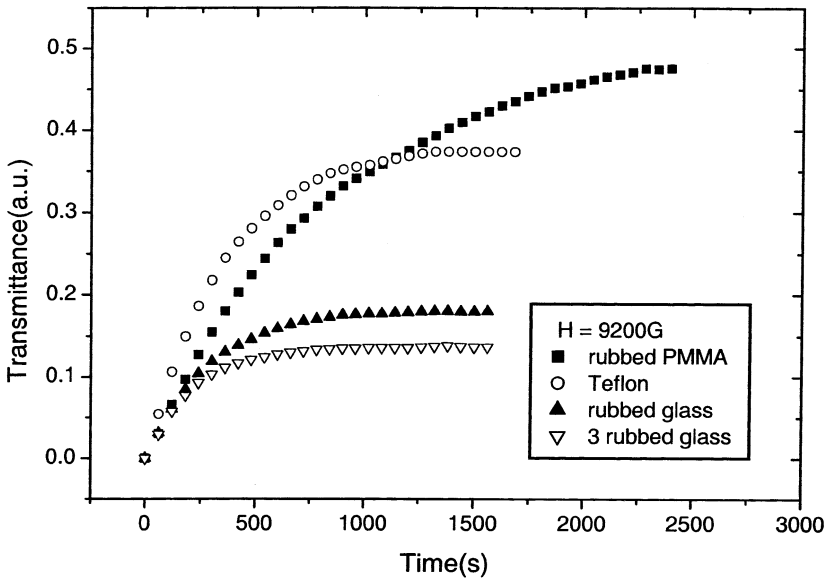

(b)

FIGURE 4 (*Continued.*)

but the orientation does not coincide with the magnetic field direction. After some hours (≈ 12 h), the cells were observed in the polarizing microscope and we verified that for the thicker sample (200 μm) the orientation induced by the magnetic field remained, but for the thinner samples (10 and 50 μm) the orientation induced by the boundary surfaces was almost recovered.

For samples 50 μm and 200 μm thick, we observed that for any magnetic field the experimental transmittance curves are superimposed for all surface treatments employed in this study. This means that, for such thickness, the interactions of the magnetic field with the bulk are much stronger than with surface interactions, and it is not possible to discriminate between the different surface treatments. Nevertheless, for the sample that is 10 μm thick, the transmittance curves show distinct behaviors depending on the surface treatments, as is shown in Figure 4(b). From these curves we can observe that the increasing of the rubbing process on the bare glass plates ("3 rubbed glass" means that the rubbing process was performed three times) leads to a lower level of saturation in the transmittance curves, indicating a smaller deformation induced by the magnetic field, and the deformation induced on the rubbed PMMA is larger than on the Teflon substrate.

We performed the fitting of the experimental curves of transmittance, using the procedure described in the theory part, with the director profile

given by Equations (2) and (3). From these fittings we can obtain the final orientation of the director in the surface, in equilibrium with the magnetic field, $\varphi_f(H)$. Using such a procedure good fittings could be achieved for the experimental curves of the thickest samples (200 μm); however, for the thinner ones (50 and 10 μm thick) the fitting was not satisfactory. These samples were examined in a polarizing microscope at different stages during the reorientation process, and it was observed that a uniform texture rotated from the initial orientation, indicating that these samples behave as a unique nematic layer gliding towards the magnetic field direction. The transmittance curves could be fitted, assuming that the orientation of the director in the whole sample is described by Equation (2) and using τ and φ_f as the fitting parameters. The quality of the fitting curves can be appreciated in Figure 4(a) for the two situations discussed above. For the 200 μm thick sample, the fitting was performed considering a twist distortion in the bulk; and for the 50 and 10 μm thick samples, we considered the sample as a unique layer gliding towards the magnetic field direction.

Equilibrium States

The values of $\varphi_f(H)$ obtained from the fitting of the experimental curves are shown in Figure 5(a) for cells prepared with substrates of rubbed PMMA and for different thickness. Since the magnetic field is applied making an angle of 45° with respect to the initial orientation, the maximum expected value of φ_f is 45°. As one could expect, the maximum gliding occurs for more intense fields, and the maximum distortion at the surface is achieved only for the thickest sample. For the 200 μm thick sample, it is possible to observe a jump of the values of φ_f for $H \gtrapprox 8000\,G$, which can be related with a breaking of the elastic coupling between the surface layer and the bulk, as discussed in the section "Reorientation of the Director in the Surface Layer." The $\varphi_f(H)$ curves (Figure 5A) could not be fitted with Equation (5). By comparing the $\varphi_f(H)$ curve of Figure 1 and the curve for 200 μm thick sample in Figure 5(a), we observe that the shape of the curves are different. The value of the critical magnetic field H_c^* is approximately the same for the nontreated and the treated substrates; $H_c^* \approx 1000\,G$, but the second critical magnetic field H_c^* presents a higher value for the treated substrate.

In the case of the samples 50 and 10 μm thick (Figure 5(a)), the maximum distortion for $H \approx 10$ kG is approximately 38° and 15°, respectively. The deformation induced by the magnetic field increases with increasing field intensity and without any discontinuity. For the sample 50 μm thick, the critical magnetic field H_c^* is $\approx 1000\,G$, whereas for the 10 μm thick H_c^* is $\approx 2000\,G$. For an applied magnetic field between 3 kG and 8 kG, the distortion induced to the 50 μm thick sample is much larger than for the

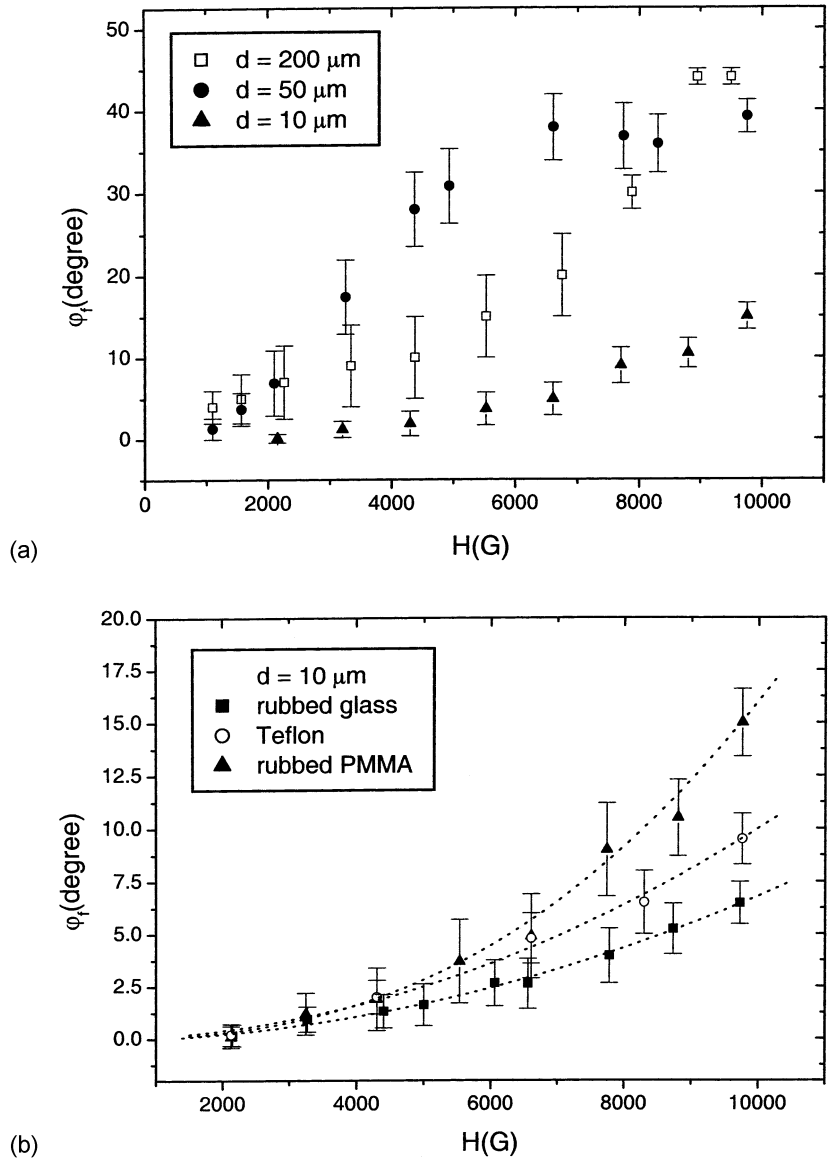

FIGURE 5 Fitted values of φ_f as a function of H, (a) in cells of different thicknesses (10, 50, and 200 μm) and (b) in cells of 10 μm thick for different surface treatments. The dashed lines are only to guide the eyes.

TABLE 1 Values of the Critical Magnetic Fields H^* and H^{**}, Comparing the Different Surface Treatments and Thicknesses

	Nontreated Substrate	Treated Substrates		
Thickness (μm)	200	200	50	10
H_c^* (G)	1000	1000	1000	2000
H_c^{**} (G)	6000	8000	—	—

200 μm thick. Nevertheless, it is important to remind that we had to assume different profiles to fit the transmittance curves; for the thick sample (200 μm) the director profile follows a continuous distortion, described by Equations (2) and (3), and for the other samples the fitting of the transmittance curves was performed by assuming that the director rotates uniformly in the whole sample towards the magnetic field.

The final configuration at the surface is approximately independent on the surface treatment for the samples 50 μm and 200 μm thick, and only for the sample 10 μm thick the curves $\varphi_f(H)$ are not superimposed for different surface treatments, as is shown in Figure 5(b). From these curves we notice that the deformation induced in the cell built with rubbed PMMA substrates is larger than the others. However, H_c^* is independent of the surface treatments and depends only on the sample thickness. In Table 1 are presented the values of H_c^* and H_c^{**} obtained directly from the experimental transmittance curves for the nontreated and treated substrates.

CONCLUSIONS

In this work we have shown that it is possible to induce a preferential alignment in a nematic lyotropic liquid crystal by surface treatments. In the case of the polymer films (rubbed PMMA and Teflon) the orientation of director coincides with the direction of the microgrooves observed by AFM, minimizing the elastic distortion [11]. Although no microgrooves were observed for the rubbed glass substrate, a good quality alignment was achieved. One possible mechanism to explain such alignment would be the separation of charge due to the rubbing. This would improve the orientation of the aggregates, with the amphiphilic molecules more strongly attached to the substrate by the polar heads.

From the transmittance curves in Figures 4(a) and 4(b) we see that the dynamic process depends on the sample thickness, and different profiles for the director evolution were used in the fitting procedure. The different surface treatments can be discriminated only using the sample 10 μm thick, where the surface effects are more evident. For the thin samples, the

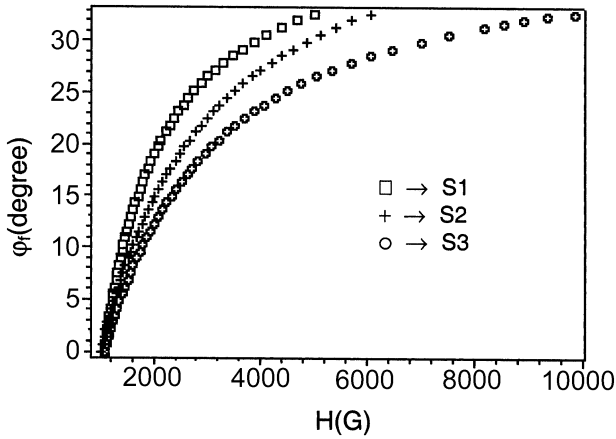

FIGURE 6 Simulated curves using Equation (5), for different values of w and l, keeping constant the other parameters. S1: $w = 10^{-4}$ erg/cm^2, $l = 7 \times 10^{-3}$ cm; S2: $w = 10^{-9}$ erg/cm^2, $l = 7 \times 10^{-3}$ cm; S3: $w = 10^{-4}$ erg/cm^2, $l = 7 \times 10^{-4}$ cm.

biaxial order induced in the surface layer propagates to the whole sample [4]; therefore there is no more difference between the surface layer and the bulk, and we can fit the experimental curves of transmittance considering that the director rotates uniformly in the whole sample, towards the magnetic field. However, the deformation induced by the magnetic field is small and the orientation induced by the substrate is recovered when the magnetic field is removed. The saturation plateau in Figure 4(b) indicates qualitatively the anchoring energy of the different substrates; therefore the anchoring would be stronger in the rubbed glass than in the rubbed PMMA.

The final configuration of the director in the surface layer was determined from the fitting of the experimental curves, and we see that the maximum distortion is achieved only in the thick sample (200 μm), with a discontinuity at $H_c^{**} \approx 8000\,G$, independent of the surface treatment. The same behavior was also observed in samples inserted in glass capillaries of the same thickness, with a lower value of H_c^{**}, as is shown in Table 1. In such capillaries, it was reported that the inner surfaces present some channels that would favor the alignment of the director in a preferential direction, and no surface treatment was applied to them.

Although the values of H_c^* are almost the same, the curves $\varphi_f(H)$ in Figures 1 and 5(a) have different shapes for $H < H_c^{**}$. Attempts to fit the experimental curves using Equation (5) were done, considering the same fitting parameters that were used to obtain the solid curve in Figure 1; however, it was not possible to find values for these parameters that could reproduce the observed dependence of φ_f on H. Simulated curves using

Equation (5) are presented in Figure 6, where we varied the parameters l and w in a large range, but we observe that the increasing of φ_f at low values of H is faster than what was observed experimentally. This point remains obscure and deserves more theoretical work.

REFERENCES

[1] Jerome, B. (1991). *Rep. Prog. Phys.*, *54*, 391.
[2] van Haaren, J. (1998). *Nature*, *392*, 331.
[3] Oliveira, E. A., Figueiredo Neto, A. M., & Durand, G. (1991). *Phys. Rev. A*, *44*, R825.
[4] Bechtold, I. H., Bonvent, J. J., & Oliveira, E. A. (2002). *Phys. Rev. E*, *65*, 011704.
[5] Lorman, V. L., Oliveira, E. A., & Metout, B. (1999). *Phys. B*, *262*, 55.
[6] Vega, L. M., Bonvent, J. J., Barbero, G., & Oliveira, E. A. (1998). *Phys. Rev. E*, *57*, R3715.
[7] Alexe-Ionescu, A. L., Vega, L. M., Bonvent, J. J., & Oliveira, E. A. (1999). *Phys. Rev. E*, *60*, 6847.
[8] Figueiredo Neto, A. M., Garlene, Y., Levelut, A. M., & Liébert, L. (1985). *J. Phys. Lett. (Paris)*, *46*, L-499.
[9] Figueiredo Neto, A. M., Levelut, A. M., Liébert, L., & Garlene, Y. (1985). *Mol. Cryst. Liq. Cryst.*, *129*, 191.
[10] Turchiello, R. de F., & Oliveira, E. A. (1996). *Phys. Rev. E*, *54*, 1618.
[11] Berreman, D. W. (1972). *Phys. Rev. Lett.*, *28*, 1683.